Phase transition of charged black holes in massive gravity through new methods

S. H. Hendi[1,2*], S. Panahiyan[1,3†], B. Eslam Panah[1‡] and M. Momennia[1§]

[1] *Physics Department and Biruni Observatory, College of Sciences, Shiraz University, Shiraz 71454, Iran*
[2] *Research Institute for Astronomy and Astrophysics of Maragha (RIAAM), P.O. Box 55134-441, Maragha, Iran*
[3] *Physics Department, Shahid Beheshti University, Tehran 19839, Iran*

Motivated by providing preliminary steps to understand the conception of quantum gravity, in this paper, we study the phase structure of a semiclassical gravitational system. We investigate the stability conditions and phase transition of charged black holes in massive gravity via canonical and geometrical thermodynamic approaches. We point out the effects of massive parameter on stability conditions of these black holes and show how massive coefficients affect the phase transition points of these black holes. We also study the effects of boundary topology on thermodynamical behavior of the system. In addition, we give some arguments regarding the role of higher dimensions and highlight the effect of the electric charge in thermodynamical behavior. Then, we extend our study to geometrical thermodynamic approach and show that it can be a successful method for studying the black hole phase transition. At last, by employing the relation between thermodynamical pressure and cosmological constant, critical behavior of the system and the effects of different parameters on critical values are investigated.

I. INTRODUCTION

Cosmological observations show that, 95% of the Universe is made of dark energy and dark matter. In order to interpret dark sector of the Universe, some various candidates have been proposed in literature, such as modified gravities like Lovelock gravity [1–3], brane world cosmology [4–8], scalar-tensor theories [9–18], and the so-called $F(R)$ gravity theories [19–35] (for a review regarding thermodynamical aspects of modified theories, see Ref. [36]). One of the interesting aspects of these theories is graviton. Graviton in the Einstein gravity is massless [37–40]. A natural question is whether one can build a self-consistent gravity theory if graviton is massive [41–43]. To do so, one should modify the Einstein theory of gravity to include massive gravitons [41–48]. From the theoretical perspective, the shear difficulty of constructing a consistent theory of massive gravity makes the problem more interesting.

Fierz and Pauli developed the ghost-free theory of non-interacting massive gravitons which had a condition of being linearized over Minkowski space [49, 50]. Then, Boulware and Deser showed that a generic extension of the Fierz-Pauli theory to curved backgrounds will contain ghost instabilities [51]. In Refs. [46, 48, 52–55], a potentially ghost-free non-linear massive gravity actions has been constructed. Furthermore, one of the classes of charged black hole solutions in nonlinear massive gravity was studied in Ref. [56]. In addition, the effective field theory of the modified gravity with massive modes has been studied in Ref. [57]. The phenomenological aspects of massive gravities with Lorentz-violation and invariant mass terms were investigated [58]. Furthermore, massive, massless and ghost modes of gravitational waves in higher order gravities were studied and the possibility of the detection and additional polarization modes of a stochastic gravitational wave were discussed in Ref. [59]. In a series of studies, the black hole solutions in different massive gravities [60–70] have been investigated and it was shown that some of these black holes may enjoy anti-evaporation in their thermodynamical properties [71, 72]. The massive gravity has also been employed to conduct some studies in the context of cosmology (for an incomplete list of these studies, we refer the reader to Refs. [73–81]). Of the other applications of massive gravity, one can point out the large applications of this gravity in the anti-de Sitter/conformal field theory (AdS/CFT) community. For example, the holographical aspects of the massive gravity coupled with nonlinear electrodynamic models have been investigated in Ref. [82]. Furthermore, the extension of massive gravities with additional couplings and higher derivative terms have been addressed and their holographical properties are extracted [83–86].

Recently, David Vegh [87] found a nontrivial black hole solution with a Ricci flat horizon in four dimensional massive gravity with a negative cosmological constant. He studied an assumption that the graviton may have lattice like behavior in the holographic conductor model: the conductivity generally exhibits a Drude peak which approaches to a delta function in the massless gravity limit. Application of massive gravity in the context of AdS/CFT correspondence via stability conditions and metal-insulator transition has been studied in [88–91]. In addition, thermodynamical

behavior and $P-V$ criticality of the Vegh's massive gravity have been, recently, investigated [92–96]. Some holographic effects of graviton mass have been investigated in Ref. [97, 98]. The main goal of this paper is to obtain Vegh's black hole solutions and study corresponding thermodynamical properties and their phase structure.

Thermodynamical aspects of the black holes and their critical behavior have been one of the greatest interests for many authors. Recently, it was proposed to change the role of some constants to the cases of (dynamical or thermodynamical) variables [99–107]. Among the thermodynamical properties of the black holes, thermal stability and phase transition have been investigated in literature. Studying thermal stability and phase transition points can be done in the context of canonical ensemble by analyzing the heat capacity. The sign of heat capacity represents stability/instability of the black holes, while its divergencies and roots are denoted as second order phase transition and bound points, respectively.

Another approach toward studying critical behavior of the black holes is through geometrical method. In this case, by employing a thermodynamical potential and corresponding extensive parameters, one can construct a phase space containing information regarding phase transition of the black holes. In other words, geometrical thermodynamics tries to introduce thermodynamical properties of the systems through the use of the Riemannian geometry. The basic motivation is to give an independent picture regarding thermodynamical aspects of systems. In addition, geometrical thermodynamics gives information regarding bound points, phase transitions, their types and stability conditions. Furthermore, it contains information regarding molecular interaction around phase transitions for the mundane systems. In other words, by studying the sign of thermodynamical Ricci scalar (TRS) around phase transition points, one can extract information whether interaction is repulsive or attractive. There are several approaches in the context of geometrical thermodynamics (GTs); the well-known metrics of the Weinhold [108, 109], Ruppeiner [110, 111] and Quevedo metric which were proposed in different structures. Recently it was pointed out that there may be some mismatches between second order phase transitions and divergencies of TRS in the mentioned methods [112–115], and an alternative thermodynamical metric was introduced to solve this problem [116–119]. The generalization of this metric in the context of extended phase space (in which constants considered as variables) was done in Ref. [120]. It was shown that thermodynamical behavior of the system in the context of extended phase space, heat capacity and GTs lead to same consequences [120]. The importance of geometrical methods comes from the fact that these methods are based on the grand canonical ensemble foundation. Although we connect this method to the heat capacity, it is worthwhile to mention that this is only for the sake of comparison and check the validity of the results.

Recent progresses in the AdS/CFT correspondence, suggest that cosmological constant should be considered as a thermodynamical variable [121–124]. In addition, in black hole thermodynamics, it was shown that such consideration could lead to remove specific thermodynamical problems such as ensemble dependency [125]. One of the corresponding thermodynamical variable for cosmological constant is pressure. It was shown that by using this analogy, one can introduce novel properties in black hole thermodynamics such as Van der Waals like behavior, triple point and reentrant of phase transition [126–135]. Therefore, by such consideration, it is possible to study critical behavior of the black holes in extended phase space. One of the new methods for extracting critical points of the black holes was proposed and employed in Ref. [120]. In this method, by using proportionality between cosmological constant and pressure in denominator of the heat capacity, a relation is obtainable for pressure which is independent of equation of state. In this paper, we will employ this method to extract critical points of the black hole system.

The outline of the paper is as follow; in section II, we review the charged massive black holes and their thermodynamical quantities. In section III, we introduce approaches for studying phase transition of these black holes in the context of heat capacity and geometrical thermodynamics, and study thermal stability of these black holes. Then, we investigate the existence of the phase transitions in the context of two mentioned approaches. The last section is devoted to closing remarks.

II. BLACK HOLE SOLUTIONS IN MASSIVE GRAVITY

The $(n+2)$-dimensional action of massive gravity with negative cosmological constant can be written as [92–95]

$$\mathcal{I} = \frac{1}{2\kappa^2} \int d^{n+2}x \sqrt{-g} \left[\mathcal{R} + \frac{n(n+1)}{l^2} - \frac{\mathcal{F}}{4} + m^2 \sum_{i=1}^{n+2} c_i \mathcal{U}_i(g, f) \right], \tag{1}$$

where $\mathcal{R}$ is the scalar curvature, $\mathcal{F}$ is the Maxwell invariant, f is a fixed rank-2 symmetric tensor and m^2 is the positive massive parameter (see Ref. [87, 136] for more details regarding the relation of positive m^2 with the wall of stability interpretation). In addition, c_i's are constants and $\mathcal{U}_i$'s are symmetric polynomials of the eigenvalues of the

$(n + 2) \times (n + 2)$ matrix $\mathcal{K}^\mu_\nu = \sqrt{g^{\mu\alpha}f_{\alpha\nu}}$ [137]

$$
\begin{aligned}
\mathcal{U}_1 &= [\mathcal{K}], \\
\mathcal{U}_2 &= [\mathcal{K}]^2 - [\mathcal{K}^2], \\
\mathcal{U}_3 &= [\mathcal{K}]^3 - 3[\mathcal{K}][\mathcal{K}^2] + 2[\mathcal{K}^3], \\
\mathcal{U}_4 &= [\mathcal{K}]^4 - 6[\mathcal{K}^2][\mathcal{K}]^2 + 8[\mathcal{K}^3][\mathcal{K}] + 3[\mathcal{K}^2]^2 - 6[\mathcal{K}^4], \\
\mathcal{U}_5 &= [\mathcal{K}]^5 - 10[\mathcal{K}]^3[\mathcal{K}^2] + 20[\mathcal{K}]^2[\mathcal{K}^3] - 20[\mathcal{K}^2][\mathcal{K}^3] + 15[\mathcal{K}][\mathcal{K}^2]^2 - 30[\mathcal{K}][\mathcal{K}^4] + 24[\mathcal{K}^5], \\
&\quad \dots .
\end{aligned}
\tag{2}
$$

The square root in $\mathcal{K}$ means $\left(\sqrt{A}\right)^\mu_\nu \left(\sqrt{A}\right)^\nu_\lambda = A^\mu_\lambda$ and $[\mathcal{K}] = \mathcal{K}^\mu_\mu$. Variation of the action (1) with respect to the metric tensor $g_{\mu\nu}$ and the Faraday tensor $F_{\mu\nu}$, leads to

$$
G_{\mu\nu} - \frac{n(n+1)}{2l^2}g_{\mu\nu} = \frac{1}{2}\left[F_{\mu\lambda}F^\lambda_\nu - \frac{1}{4}g_{\mu\nu}\mathcal{F}\right] + m^2\chi_{\mu\nu},
\tag{3}
$$

$$
\nabla_\mu F^{\mu\nu} = 0,
\tag{4}
$$

where $G_{\mu\nu}$ is the Einstein tensor and

$$
\begin{aligned}
\chi_{\mu\nu} &= -\frac{c_1}{2}\left(\mathcal{U}_1 g_{\mu\nu} - \mathcal{K}_{\mu\nu}\right) - \frac{c_2}{2}\left(\mathcal{U}_2 g_{\mu\nu} - 2\mathcal{U}_1\mathcal{K}_{\mu\nu} + 2\mathcal{K}^2_{\mu\nu}\right) - \frac{c_3}{2}(\mathcal{U}_3 g_{\mu\nu} - 3\mathcal{U}_2\mathcal{K}_{\mu\nu} + \\
&\quad 6\mathcal{U}_1\mathcal{K}^2_{\mu\nu} - 6\mathcal{K}^3_{\mu\nu}) - \frac{c_4}{2}(\mathcal{U}_4 g_{\mu\nu} - 4\mathcal{U}_3\mathcal{K}_{\mu\nu} + 12\mathcal{U}_2\mathcal{K}^2_{\mu\nu} - 24\mathcal{U}_1\mathcal{K}^3_{\mu\nu} + 24\mathcal{K}^4_{\mu\nu}) + \dots .
\end{aligned}
\tag{5}
$$

We take into account the metric of $(n + 2)$-dimensional spacetime with the following form

$$
ds^2 = -f(r)dt^2 + f^{-1}(r)dr^2 + r^2 h_{ij}dx_i dx_j, \;\; i, j = 1, 2, 3, ..., n
\tag{6}
$$

where $h_{ij}dx_i dx_j$ is the line element for an $n-$dimensional Einstein space with constant curvature $n(n + 1)k$ and volume V_n. We should note that the constant k indicates that the boundary of $t = constant$ and $r = constant$ can be a positive (elliptic), zero (flat) or negative (hyperbolic) constant curvature hypersurface.

A generalized version of $f_{\mu\nu}$ was proposed in Ref. [92–95] with the following form

$$
f_{\mu\nu} = diag(0, 0, c_0^2 h_{ij}),
\tag{7}
$$

where by employing it, the metric function $f(r)$ will be [92, 93]

$$
\begin{aligned}
f(r) &= k + \frac{r^2}{l^2} - \frac{m_0}{r^{n-1}} + \frac{q^2}{2n(n-1)r^{2(n-1)}} + \frac{c_0 c_1 m^2}{n}r + c_0^2 c_2 m^2 + \\
&\quad (n-1)c_0^3 c_3 m^2 r^{-1} + (n-1)(n-2)c_0^4 c_4 m^2 r^{-2} + \dots ,
\end{aligned}
\tag{8}
$$

in which m_0 and q are integration constants which are related to the total mass and electric charge of the black hole, respectively. As one can see, the massive terms could be up to $n + 2$ number. Technically, it is not easy to study the total behavior of the solutions with this number of terms. Therefore, for the simplicity, we restrict our study to $\mathcal{U}_i$ up to the fourth term, $\mathcal{U}_4$ [153].

In order to study the effects of massive gravity, one can investigate the metric function. Regarding various terms of $f(r)$, it is worthwhile to mention that fourth term (q^2 term) is dominant near the origin and therefore one can conclude that the singularity is timelike. In addition, for large distance, second term (r^2/l^2 term) is dominant which confirms that the solutions are asymptotically adS. It is evident that the behavior of the metric function is highly sensitive to massive parameters and contribution of the massive gravity (see Figs. 2 and 3). For specific values of different parameters, the total behavior of the metric function will be similar to the metric function of Einstein-Maxwell gravity which is containing two roots, one extreme root or without any root (see Fig. 1). Whereas by considering other choices of free parameters, the following configurations for the roots of the metric function may happen. For example, two extreme roots (dashed line in Fig. 2), three roots in which the smaller one is extreme (dotted line in Fig. 2), four roots (bold-dotted line in Fig. 2), three roots where the bigger one is extreme (continues line in Fig. 2) and three roots which the middle one is extreme (bold continues line in Fig. 2). As one can see, these different behaviors are originated from contributions of the massive gravity. The existence of multi-horizon for massive gravity
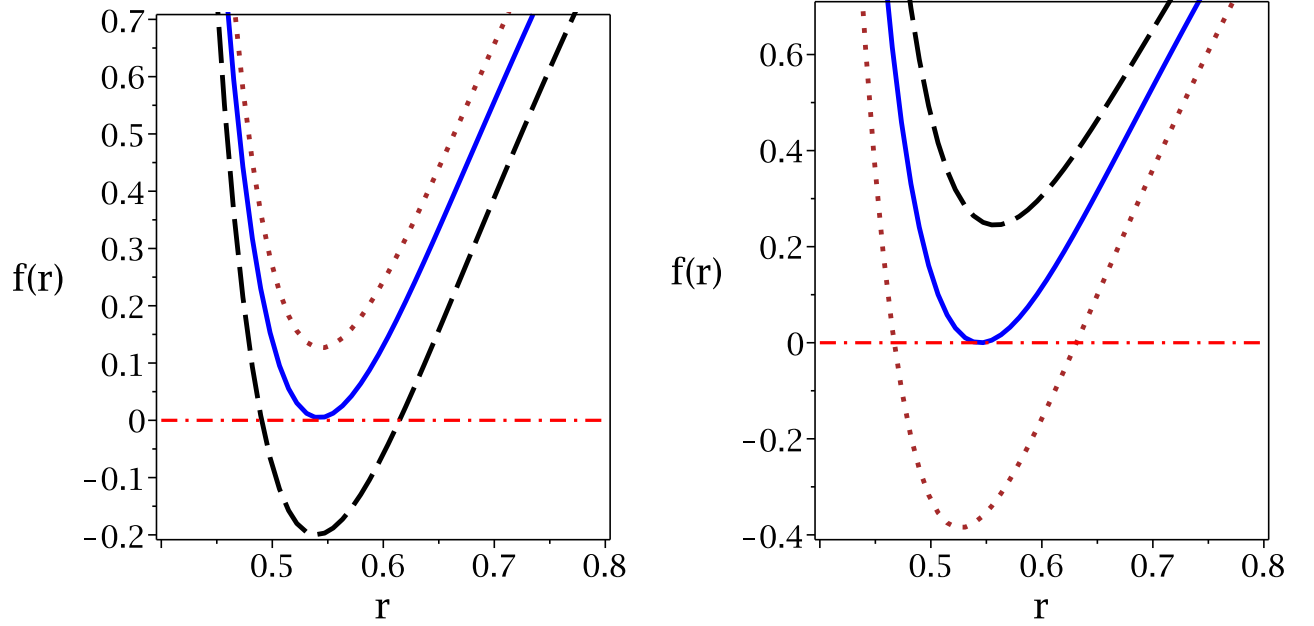
FIG. 1: $f(r)$ versus r for $l = 1$, $q = 1$, $c_0 = 0.1$, $c_1 = -0.3$, $c_2 = 2$, $c_3 = 3$, $c_4 = 2$, $k = 1$ and $n = 4$.
Left diagram for $m_0 = 0.5$, $m = 0.3$ (dashed line), $m = 2.38$ (continues line) and $m = 3$ (dotted line).
Right diagram for $m = 2$, $m_0 = 0.45$ (dashed line), $m_0 = 0.49$ (continues line) and $m_0 = 0.55$ (dotted line).
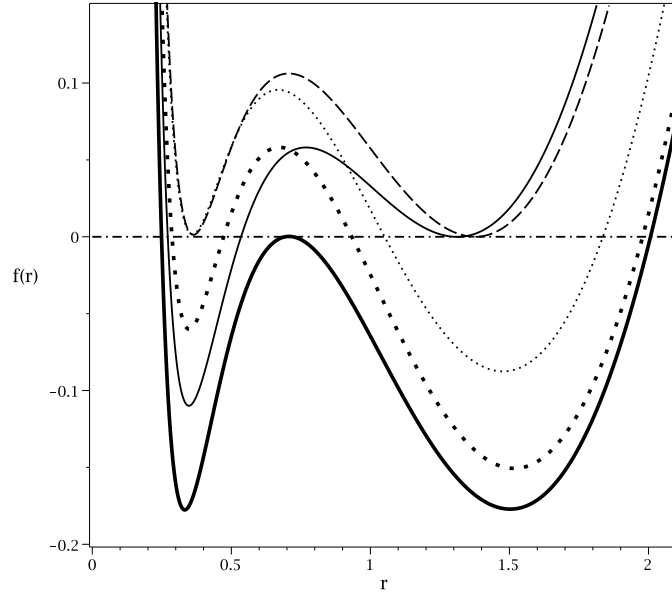

FIG. 2: $f(r)$ versus r for $l = 1$, $q = 1$, $c_0 = 0.1$, $c_1 = -2.3$, $c_2 = 10$, $k = 1$, and $n = 2$.
Diagrams for $m_0 = 1.648$, $m = 5.50$ (dashed line), $m_0 = 1.668$, $m = 5.60$ (dotted line), $m_0 = 1.70$, $m = 5.65$ (bold-dotted line),
$m_0 = 1.68$, $m = 5.462$ (continues line) and $m_0 = 1.74$, $m = 5.65$ (bold line).

has been reported in Refs. [71, 72] as well. It was shown that the existence of such property with specific quantum corrections leads to a phenomena which is opposite of the black holes evaporation. In other words, there might exist an anti-evaporation behavior for the black holes in these cases. Here, we see that similar property is observed for these black holes. Therefore, it is possible that anti-evaporation property exists for these black holes in the presence of massive gravity. It is worthwhile to mention that anti-evaporation has been reported for specific black holes in $F(R)$ gravity as well [138–140].

Considering the fact that we are interested in studying GTs and heat capacity of the solutions, we give a brief
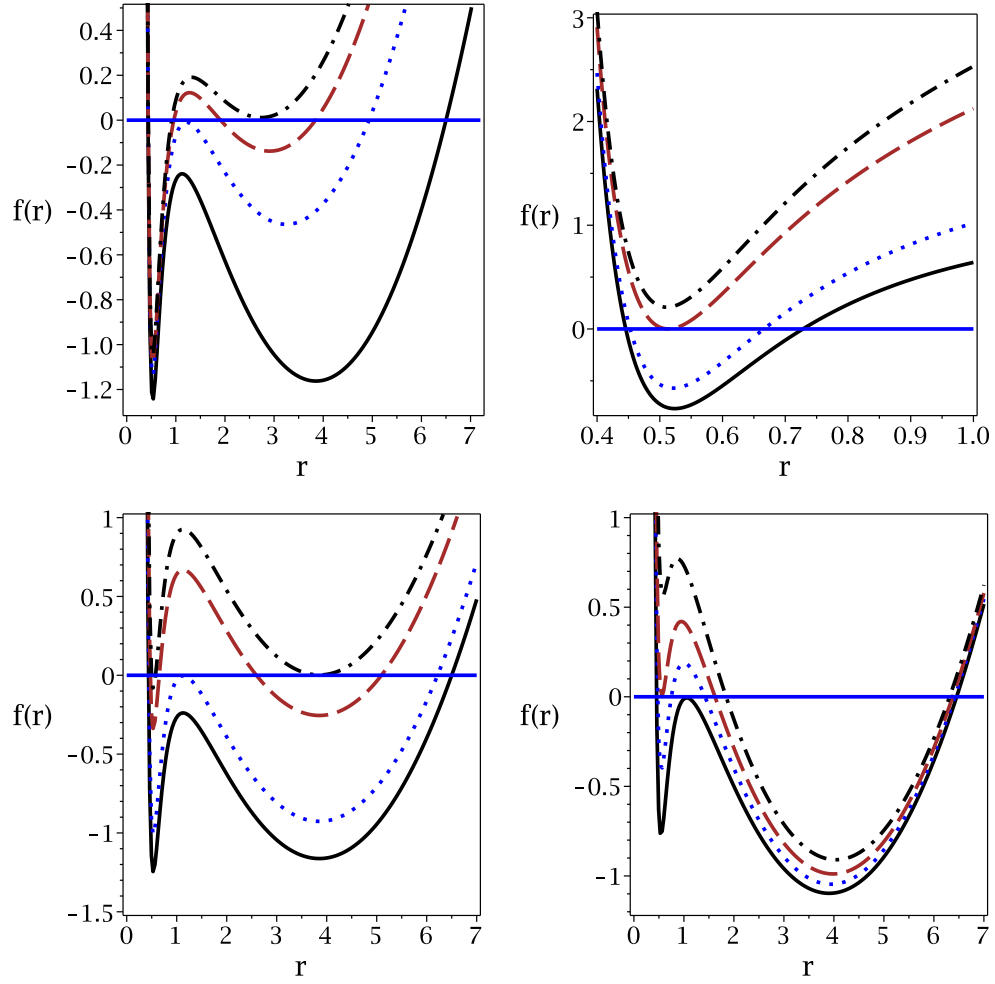
FIG. 3: $f(r)$ versus r for $l = 1$, $q = 1$, $c_0 = 0.1$, $c_4 = 1$, $k = 1$, $m_0 = 0.6$, $m = 5.5$ and $n = 4$.
Left-up panel: for $c_2 = c_3 = 1$, $c_1 = -1.7$ (continuous line), $c_1 = -1.44$ (dotted line), $c_1 = -1.3$ (dashed line) and $c_1 = -1.23$ (dashed-dotted line).
Right-up panel: for $c_2 = c_3 = 1$, $c_1 = -0.5$ (continuous line), $c_1 = 0$ (dotted line), $c_1 = 1.46$ (dashed line) and $c_1 = 2$ (dashed-dotted line).
left-down panel: for $c_1 = -1.7$, $c_3 = 1$, $c_2 = 1$ (continuous line), $c_2 = 1.78$ (dotted line), $c_2 = 4$ (dashed line) and $c_2 = 4.85$ (dashed-dotted line).
right-down panel: for $c_1 = -1.7$, $c_2 = 1$, $c_3 = 3.8$ (continuous line), $c_3 = 6$ (dotted line), $c_3 = 8.5$ (dashed line) and $c_3 = 12$ (dashed-dotted line).

review about the conserved charges and thermodynamic quantities in which they have been obtained in Ref. [92].

Regarding the obtained solutions, the action (1) diverges, as is the Hamiltonian and other associated conserved quantities. One of the systematic methods for removing this divergency is through the use of the counterterm method inspired by AdS/CFT correspondence [141–144]. It was also shown that by using the Hamiltonian approach, one can find the mass M of the black hole solutions as (see Ref. [92] for more details)

$$M = \frac{nV_n}{2\kappa^2}m_0.$$ (9)

In addition, the electric charge of the black hole, Q, can be obtained by using the Gauss's law and calculating the electromagnetic flux at infinity. Straightforward calculations lead to the following result

$$Q = \frac{V_n}{2\kappa^2}q.$$ (10)

The temperature may be obtained through the use of regularity of the solutions at the event horizon (the largest

root of metric function which is denoted by r_+). It is also calculated through the use of the surface gravity definition as

$$T = \frac{1}{2\pi} \sqrt{-\frac{1}{2} \left(\nabla_\mu \chi_\nu\right) \left(\nabla^\mu \chi^\nu\right)},$$

where $\chi = \partial_t$ is the Killing vector. It is easy to show that [92]

$$
\begin{aligned}
T = \frac{1}{4\pi r_+} & \left[(n-1)k + (n+1)\frac{r_+^2}{l^2} - \frac{q^2}{2nr_+^{2(n-1)}} + c_1 c_0 m^2 r_+ (n-1)c_2 c_0^2 m^2 + \right. \\
& \left. \frac{(n-1)(n-2)c_3 c_0^3 m^2}{r_+} + \frac{(n-1)(n-2)(n-3)c_4 c_0^4 m^2}{r_+^2} \right],
\end{aligned}
$$

(11)

where r_+ satisfy $f(r = r_+) = 0$.

At last, we should obtain the entropy of the black hole solutions. The entropy of the black holes satisfies the so-called area law [145–150] in the context of Einstein gravity. According to this law, one finds that the black hole entropy is equal to one-quarter of the horizon area, i.e.,

$$S = \frac{2\pi V_n}{\kappa^2} r_+^n.$$

(12)

III.   GEOMETRICAL STUDY OF THE PHASE TRANSITION AND THERMAL STABILITY

In this section, we study the local stability and second order phase transition of the solutions in the canonical ensemble and compare our results with a new GTs approach for the phase transition and bound points.

In the canonical ensemble, the positivity of the heat capacity is sufficient to ensure thermal stability. One can calculate the heat capacity as

$$C_Q = T \left(\frac{\partial S}{\partial T}\right)_Q = \frac{\left(\frac{\partial M}{\partial S}\right)_Q}{\left(\frac{\partial^2 M}{\partial S^2}\right)_Q}.$$

(13)

Considering the fact that changing in the sign of heat capacity is representing the phase transition between unstable/stable states, we regard divergence points of the heat capacity as second order phase transition points. So, the second order phase transition and bound points of the black holes with regular T in the context of heat capacity are indicated with following relations

$$
\begin{cases}
T = \left(\frac{\partial M}{\partial S}\right)_Q = 0 & bound \ point \\
\\
\left(\frac{\partial^2 M}{\partial S^2}\right)_Q = 0 & phase \ transition \ point
\end{cases}
,
$$

(14)

where we called the roots and divergence points of the heat capacity as bound points and (second order) phase transition points, respectively. It is notable that $T = 0$ indicates a bound point between nonphysical ($T < 0$) and physical ($T > 0$) region.

On the other hand, GTs is another way for investigating the phase transition in the context of black hole thermodynamics. In this approach, several metrics have been introduced (Ruppeiner, Weinhold and Quevedo metrics) in which by using of these metrics, one can investigate the phase transition of black holes. It was previously shown that these metrics encounter with some problems for specific types of black holes [116–119]. Recently, a new metric (HPEM metric) was proposed in order to solve the problems that other metrics may confront [116–119]. The roots of denominator of the Ricci scalar of HPEM metric only contains the roots of numerator and denominator of the heat capacity. In other words, divergence points of the Ricci scalar of HPEM metric only coincide with the roots and divergence points of the heat capacity. The HPEM metric has the following form

$$ds^2_{HPEM} = \frac{SM_S}{\left(\Pi_{i=2}^n \frac{\partial^2 M}{\partial \chi_i^2}\right)^3} \left(-M_{SS}dS^2 + \sum_{i=2}^n \left(\frac{\partial^2 M}{\partial \chi_i^2}\right) d\chi_i^2\right),$$

(15)

where $M_S = \partial M/\partial S$, $M_{SS} = \partial^2 M/\partial S^2$ and χ_i $(\chi_i \neq S)$ are extensive parameters. In what follows, we will study the stability and second order phase transition of the charged massive black holes in the context of heat capacity and GTs.

First of all, one should take this fact into consideration that the sign of temperature is putting a restriction on systems to be physical or non-physical. As we see later, there will be a critical horizon radius, r_{+c}, in which for $r_+ < r_{+c}$ the temperature of the system is negative and in this region solutions are non-physical.

It is a matter of calculation to show that for the root of the heat capacity, one can find following relation with respect to the massive parameter

$$m_c \equiv m|_{C_Q=0} = \frac{1}{2l} \sqrt{\frac{A}{B}}, \tag{16}$$

where

$$A = 2 \left[q^2 l^2 - 2n \left(n + 1 \right) r_+^{2n} \right] r_+ - 4nl^2 k r_+^{2n-4}, \tag{17}$$

$$B = nc_0 r_+^{2n-4} \left[c_0 c_2 \left(n - 1 \right) r_+^2 + c_1 r_+^3 + \left(n - 1 \right) \left(n - 2 \right) c_0^2 \left\{ r_+ c_3 + c_0 c_4 \left(n - 3 \right) \right\} \right]. \tag{18}$$

Regarding positive c_i leads to positive B and therefore, we should restrict the parameters to obtain positive A. The limitation reduces to the following inequality

$$q^2 l^2 - 2knl^2 r_+^{2n-5} - 2n \left(n + 1 \right) r_+^{2n} > 0,$$

where for the flat boundary $(k = 0)$, one finds

$$r_+ < \left(\frac{q^2 l^2}{2n \left(n + 1 \right)} \right)^{\frac{1}{2n}}.$$

It is worthwhile to mention that in the absence of massive parameter $(m = 0)$, the obtained solutions will reduce to Reissner–Nordström black holes and these black holes only enjoy bound point. Here, in the presence of massive gravity $(m \neq 0)$, there is also only one root for heat capacity, which is a function of the massive parameter. It is notable that massive coefficients (c_i's), are only presented in denominator of the obtained critical value. Therefore, in case of $c_i > 1$, the effects of these coefficients on the critical value of massive parameter, are of decreasing ones. Whereas for the case of $0 < c_i < 1$, their effects are in favor of increasing the value of the critical massive parameter. In other words, they increase the value of m_c.

Next, as for the divergence points of the heat capacity, hence second order phase transitions, we find following critical relation for the massive parameter

$$m_i \equiv m|_{C_Q \longrightarrow \infty} = \frac{1}{2lc_0} \sqrt{\frac{C}{D}}, \tag{19}$$

in which

$$C = 6 \left[\left(2n - 1 \right) q^2 l^2 + 2n \left(n + 1 \right) r_+^{2n} \right] r_+ - 12kl^2 n \left(n - 1 \right) r_+^{2n-2}, \tag{20}$$

$$D = 3n \left(n - 1 \right) r_+^{2n-4} \left[r_+^2 c_2 + c_0 \left(n - 2 \right) \left\{ 2r_+ c_3 + 3c_0 c_4 \left(n - 3 \right) \right\} \right]. \tag{21}$$

It is evident that in this case, similar to the case of heat capacity's root, due to structure of the square root functions, there will be some restrictions. Interestingly, in this case for $k = 0$ and $k = -1$ and due to our interest only in positive values of massive coefficients, C and D are always positive and there is no restriction. Whereas for the case of spherical symmetric, there is only one restriction which is in the following form

$$\left(2n - 1 \right) q^2 l^2 + 2n \left(n + 1 \right) r_+^{2n} - 2l^2 n \left(n - 1 \right) r_+^{2n-3} > 0, \tag{22}$$

in which due to its complexity it was not possible to find an analytical restriction with respect to horizon radius. Another interesting property of the obtained equation for the divergence points of the heat capacity is the independency of the critical massive parameter of the c_1 coefficient. In other words, critical value of the massive parameter in case of divergencies of the heat capacity is independent of the variation of c_1. Therefore, there is no contribution of the c_1 to critical value of the massive parameter. It is worthwhile to mention that, in this case similar to root of the heat
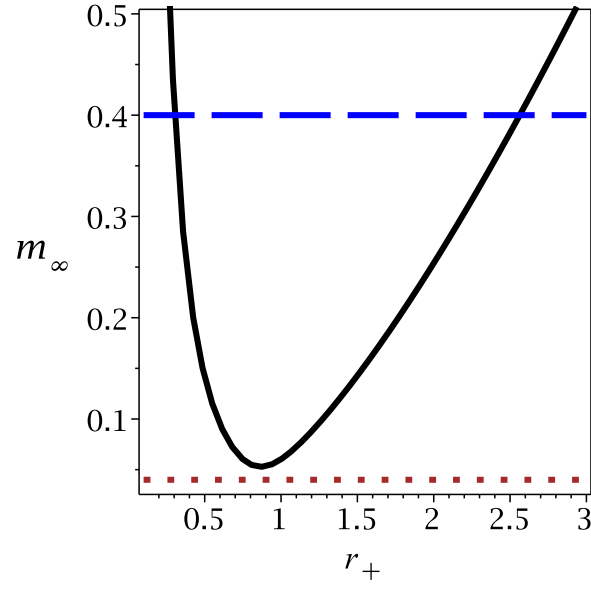
FIG. 4: m_i (continues line) versus r_+ for $l = q = 1$, $c_0 = c_2 = c_3 = c_4 = 2$, $n = 4$, and $k = 1$. $m_i = 0.04$ (dotted line) $m_i = 0.4$ (dashed line)
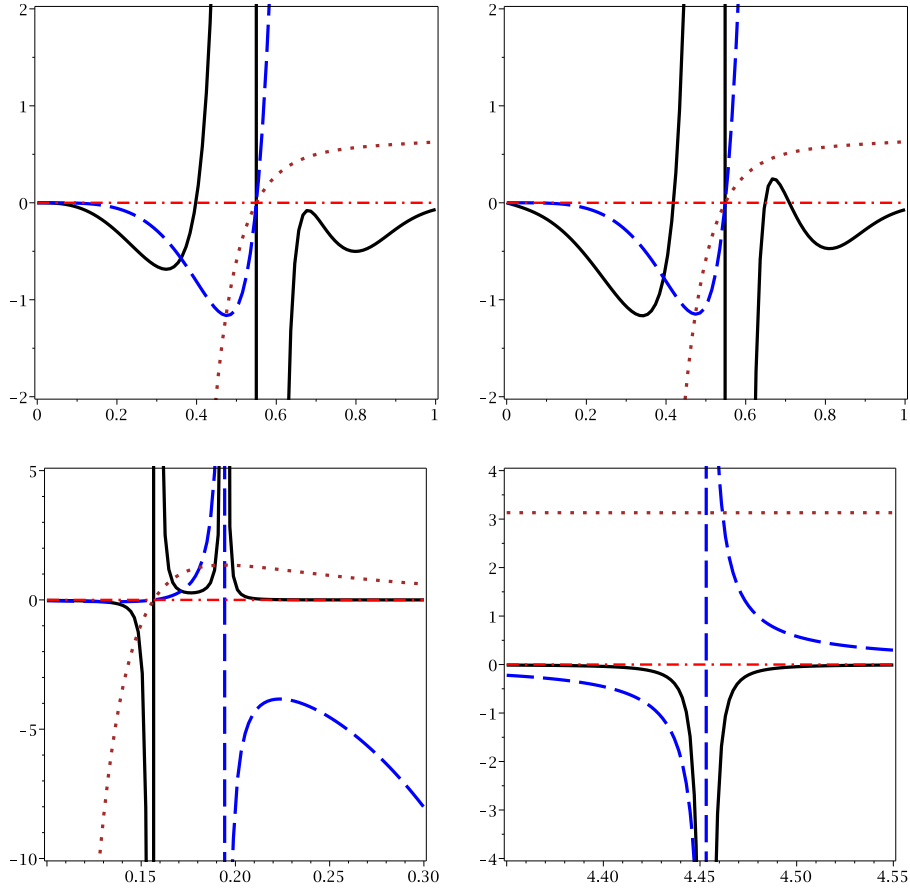

FIG. 5: $\mathcal{R}$ (continuous line), C_Q (dashed line) and T (dotted line) versus r_+ for $l = q = 1$, $c_0 = c_1 = c_2 = c_3 = c_4 = 2$, $n = 4$, and $k = 1$; $m = 0$ (up - left), $m = 0.01$ (up - right) and $m = 1$ (down panels with different scales).
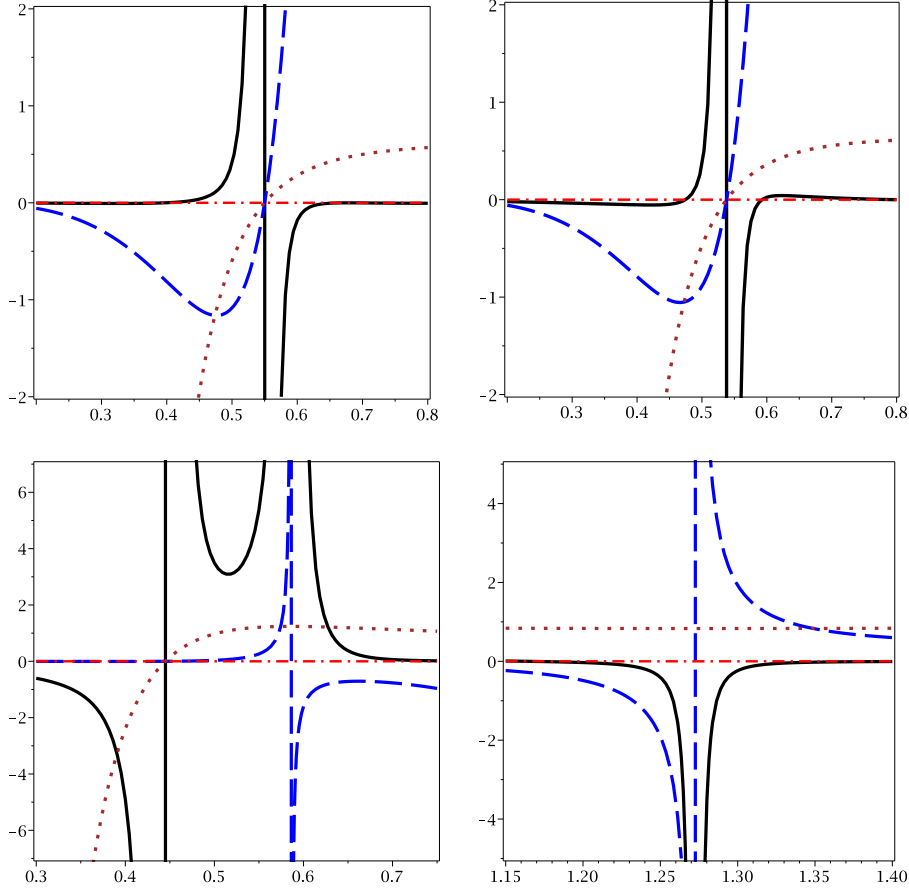
FIG. 6: $\mathcal{R}$ (continuous line), C_Q (dashed line) and T (dotted line) versus r_+ for $l = q = 1$, $c_1 = c_2 = c_3 = c_4 = 2$, $n = 4$, $m = 0.1$ and $k = 1$; $c_0 = 0$ (up - left), $c_0 = 1$ (up - right) and $c_0 = 2$ (down panels with different scales).

capacity, the presences of the massive coefficients are only observed in denominator of m_i. Therefore, similar effects for variation of the massive coefficients in case of root of heat capacity will be observed in this case too.

In addition, it must be pointed out that the obtained value of massive parameter in Eq. (19) is not an injective function. Plotting m_i with respect to horizon radius, one finds that there is a value of m_i, say m_{i_C} in which for $m_i < m_{i_C}$, there will be no critical horizon radius available. In other words, in this region there is no divergence point for the heat capacity. In case of $m_i = m_{i_C}$, there will be only one divergence point for heat capacity and finally for the case of $m_i > m_{i_C}$, there will be two horizon radii for any critical value of the massive parameter. This property of the obtained equation will be shown in the plotted graphs for the heat capacity. Here, in order to elaborate mentioned behavior for Eq. (19), we have plotted Fig. 4.

Next, by employing the Eqs. (11), (13) and (15), we plot Figs. 5-8 to study thermodynamic and geometrical thermodynamic behavior of these black holes.

It is evident that for the small values of massive parameter, there is no second order phase transition (Fig. 5 up). Whereas for large values of this parameter, there is a bound point and a second order phase transition (Fig. 5 down). It is worthwhile to mention that this behavior could be observed by studying Fig. 4. Also, according to the plotted graph for m_i (Fig. 4), the smaller (larger) divergence point of the heat capacity is a decreasing (an increasing) function of m. This behavior is also evident from plotted graphs for variation of m (Fig. 5).

Besides, due to coupling of different powers of c_0 with massive parameter, we have studied the effects of variation of this coefficient. Interestingly, similar to behavior of the massive parameter, for small values of c_0, only a bound point is observed (Fig. 6 up). It is seen that only for sufficiently large values of this coefficient, two second order phase transitions and a bound point are obtained (Fig. 6 down).

Our next effects of interest are due to variation of topology of the solutions. If we denote the indexes F, H and S as representing flat ($k = 0$), hyperbolic ($k = -1$) and spherical horizons respectively, and also root of heat capacity with r_0 and two divergence points of the heat capacity with r_{Div1} (smaller one) and r_{Div2} (larger one), we can find
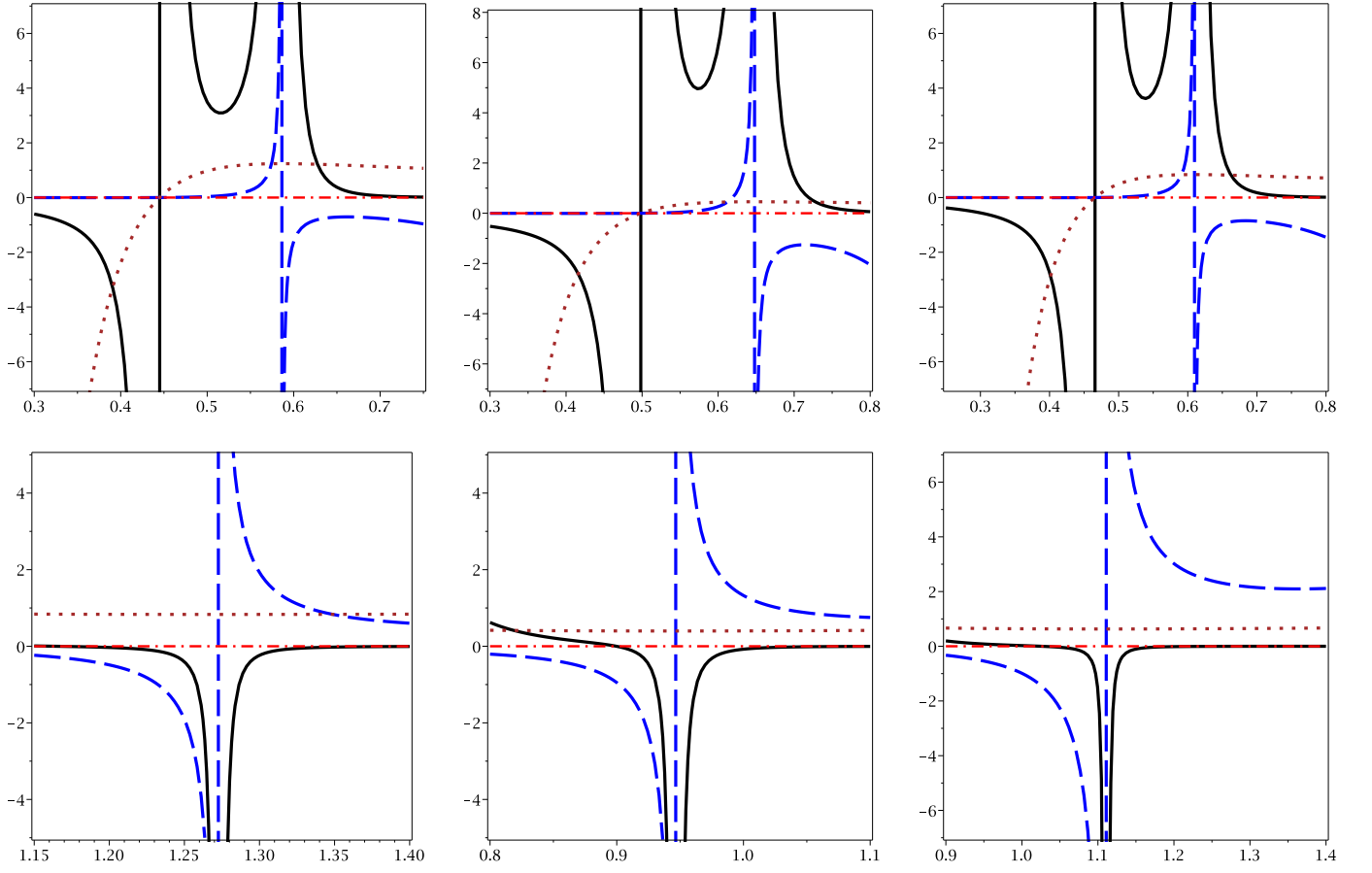
FIG. 7: $\mathcal{R}$ (continuous line), C_Q (dashed line) and T (dotted line) versus r_+ for $l = q = 1$, $c_0 = c_1 = c_2 = c_3 = c_4 = 2$, $n = 4$, and $m = 0.1$; for different scale: $k = 1$ (left panels up and down), $k = -1$ (middle panels up and down) and $k = 0$ (right panels up and down).
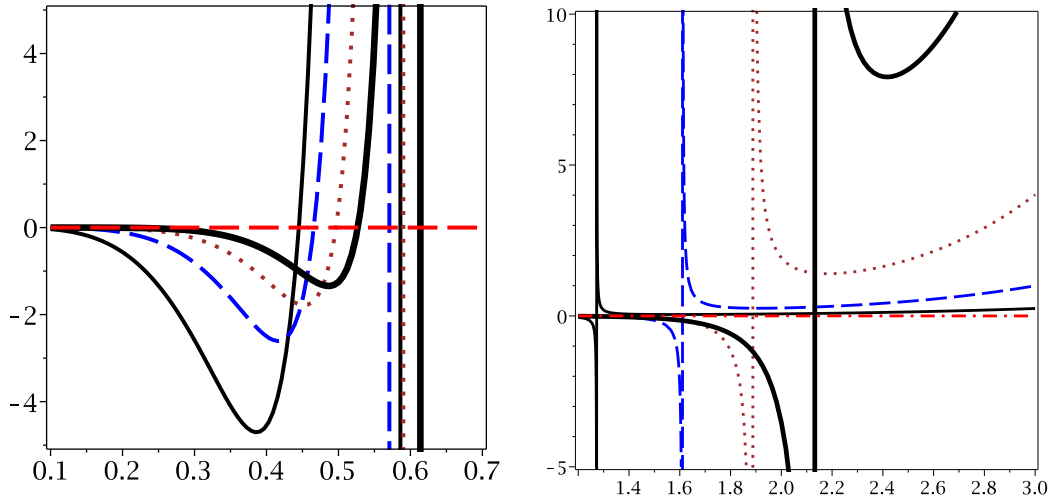

FIG. 8: C_Q versus r_+ for $l = q = 1$, $c_0 = c_1 = c_2 = c_3 = c_4 = 2$, $k = 1$, and $m = 0.1$.
for different scales: $n = 4$ (continues line), $n = 5$ (dashed line), $n = 6$ (dotted line) and $n = 7$ (bold continues line).
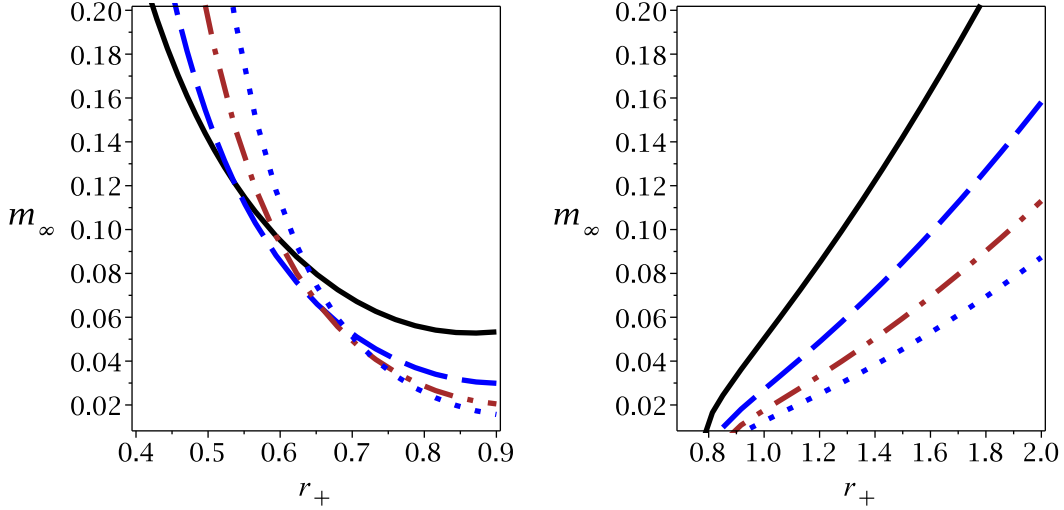
FIG. 9: m_i (continues line) versus r_+ for $l = 1$, $c_0 = c_1 = c_2 = c_3 = c_4 = 2$, $k = 1$, $n = 4$ (continues line), $n = 5$ (dashed line), $n = 6$ (dashed-dotted line) and $n = 7$ (dotted line); $q = 1$ (left panel) and $q = 0$ (right panel)

following results. For the root of the heat capacity, we have $r_{0-S} < r_{0-F} < r_{0-H}$. In other words, the highest value for the root of heat capacity belongs to the solutions with hyperbolic topology. In addition, one can find that $r_{Div1-S} < r_{Div1-H} < r_{Div1-F}$ which indicates that the highest value of smaller divergence point belongs to flat horizon (Fig. 7 up). Finally, for the larger divergence point, one can find that $r_{Div1-H} < r_{Div1-F} < r_{Div1-S}$ which means that in this case the highest value of larger divergence point belongs to spherical symmetric black holes (Fig. 7 down).

Finally, we are in a position to study the effects of dimensions on thermodynamical behavior of the system. In plotted graph, we only present the heat capacity diagrams for various dimensions. Evidently the root of the heat capacity is only an increasing function of dimensions (Fig. 8 left). As for divergence point of the heat capacity, the larger one is also an increasing function of dimensions (Fig. 8 right). But regarding the smaller divergence point, interestingly, an anomaly is observed in case of $n = 5$. In other words, for increasing value of dimensions, the smaller divergence point increases except for the case of $n = 5$ which its smaller divergence point is smaller than the case of $n = 4$. In order to find the reason for this behavior, once again we plot Fig. 9 (left) for different dimensions. Evidently, for specific small values of m, the behavior of the system is with order, in which increment in dimensions leads to increase in value of the smaller divergence point of the heat capacity. On the other hand, for special values of m the smaller divergence points of different dimensions will be the same. In other words, there are some values of m in which smaller divergence point of the heat capacity will be the same for $n = 4$ and $n = 5$ or other dimensions. This behavior of the system is solely because of the structure of m_i, and it is the characteristic behavior of the system with this configuration (for this type of massive gravity). It is worthwhile to mention that increasing the value of dimensions will decrease the region in which there is no second order phase transition. In other words, the minimum of the m_i is a decreasing function of dimensions. Interestingly, for the case of vanishing electric charge (Fig. 9 right), the mentioned behavior will not be seen. In this case, there is only one second order phase transition for these black holes which specifies the role of the electric charge in thermodynamical behavior of the system.

Now, we focus to study thermal stability of the solutions. The stability of the solutions, hence, thermodynamical behavior of these black holes are presented by the bound point and number of the second order phase transitions. For example, in case of only one bound point (up panels of Figs. 6 and 7), there is a region in which both temperature and heat capacity are negative. Therefore, this region is presenting the non-physical unstable state for black holes. After passing the bound point, the system acquires a stable physical state. For the cases of two second order phase transitions and one bound point (down panels of Figs. 6 and 7), there are several changes in the sign of heat capacity. By using naming that was used before, one can find that for the case of $r_+ < r_0$, system is in nonphysical and unstable phase. Whereas in $r_+ = r_0$ system goes under a transition from nonphysical to physical state and for $r_0 < r_+ < r_{Div1}$, system is in thermally stable state with positive temperature. As for the $r_{Div1} < r_+ < r_{Div2}$, system is in unstable state and for $r_{Div2} < r_+$, black holes are thermally stable with positive temperature. Therefore, due to thermodynamical concept in which system desires to find stable state, there are two second order phase transitions. For the case of $r_+ = r_{Div1} + \delta$, in which δ is so small, the system goes under a second order phase transition from larger unstable black hole to smaller stable black hole. In other words, in this phase transition the size of the black

hole decreases. On the other hand, for the case of $r_+ = r_{Div2} - \delta$, black hole in this configuration goes under another second order phase transition. In this one, black hole acquires larger horizon radius, hence its size increases.

Next, we study the geometrical thermodynamic behavior of the system. Figs. 5 to 8 show that considered metric in the context of GTs, provided a successful machinery. In other words, bound point and second order phase transitions for the heat capacity and the divergence points of Ricci scalar of the considered metric coincide with each other. Therefore, the mentioned metric has divergencies in place of bound point as well as second order phase transition points. On the other hand, the behavior of the Ricci scalar near bound point and second order phase transitions is not the same. For the root of the heat capacity (bound point) the sign of TRS is different for before and after that point. Whereas, in case of the second order phase transition, the sign of TRS is fixed. This change in sign enables one to distinguish bound point from second order phase transition. Therefore, it is possible to find bound point and phase transition by applying GTs, without the use of heat capacity diagrams.

IV.   CRITICAL BEHAVIOR IN EXTENDED PHASE SPACE

A.   critical behavior in extended phase space through usual method

The van der Waals like behavior of the black holes could be studied through the use of the analogy between cosmological constant and thermodynamical pressure. The proportionality between cosmological constant and pressure is given by

$$P = -\frac{\Lambda}{8\pi}. \tag{23}$$

By replacing the cosmological constant with thermodynamical pressure in temperature, one can obtain the equation of state. Using this equation of state and inflection point property, one can extract critical points and study van der Waals like behavior. For black hole solutions which considered in this paper, the critical behavior of the system through usual method has been investigated in Ref. [93]. Here, we would like to investigate the critical properties of the black holes through a new method.

B.   critical behavior in extended phase space through new method

In this section, we will study the critical behavior of these black holes through the use of the proportionality between pressure and cosmological constant. The method which we employ to do so, was introduced in Ref. [120]. By replacing the cosmological constant with its corresponding thermodynamical pressure in the heat capacity, one is able to obtain a relation for the pressure by solving the denominator of heat capacity. The maximum of $P(r_+)$ is where the second order phase transition takes place. In this relation, P does not explicitly depend on the temperature, and therefore, this relation differs from equation of state, but it contains all the information regarding phase structure of the black holes. For the pressures smaller than critical pressure, two horizon radii for each pressure exist which indicate three phases. While for pressures larger than critical pressure, no phase transition is observable.

Using the denominator of heat capacity (13) with (23), one can find following relation for the pressure

$$P = \frac{3n(n-1)^2(n-2)(n-3)c_0^4 m^2 c_4}{16\pi r_+^4 (1+n)} + \frac{n(n-1)^2(n-2)c_0^3 m^2 c_3}{8\pi r_+^3 (1+n)} + \frac{n(n-1)^2 c_0^2 m^2 c_2}{16\pi r_+^2 (1+n)} - \frac{(n-1)(2n-1)q^2}{32\pi r_+^{2n}(1+n)} + \frac{kn(n-1)^2}{16\pi r_+^2 (1+n)}. \tag{24}$$

In order to find the critical horizon radius, one should calculate first order derivation of the pressure with respect to horizon radius and solve it for r_+. Calculations show that it is not possible to obtain critical horizon radius analytically. Therefore, we employ numerical method. The results are presented in various diagrams (Figs. 10-12). In addition, we have plotted coexistence curve which characterizes two different phases of small/larger black holes with same temperature and pressure.

Evidently, due to the existence of maximum for pressure, these black holes enjoy second order phase transition in their phase space. The critical pressure and temperature are increasing functions of the massive parameter (Fig. 10), c_0 (Fig. 11) and dimensions (Fig. 12). As for critical horizon radius, it is a decreasing function of the massive parameter (left panel of Fig. 10) and c_0 (left panel of Fig. 11) while it is an increasing function of dimensions (left
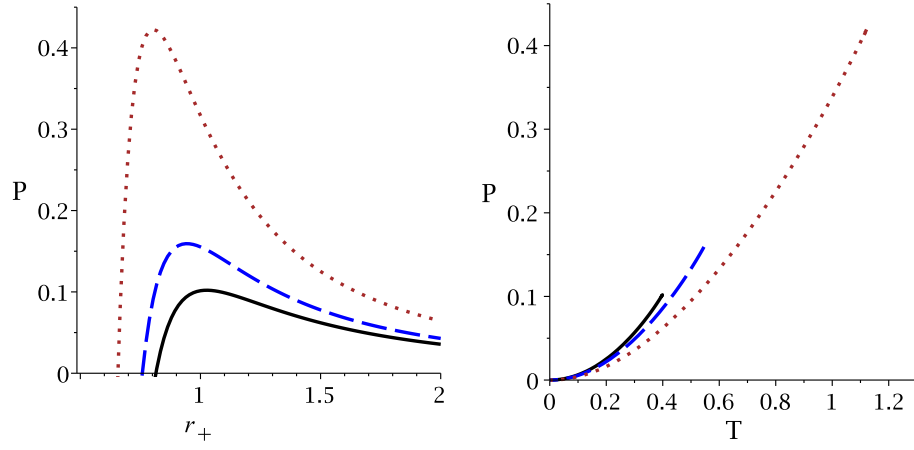
FIG. 10: P versus r_+ (left panel) and P versus T (right panel) for $c_0 = c_1 = c_3 = c_4 = 2$, $c_2 = 3$ $k = 1$, $q = 1$ and $n = 4$; $m = 0$ (continues line), $m = 0.1$ (dashed line) and $m = 0.2$ (dotted line).
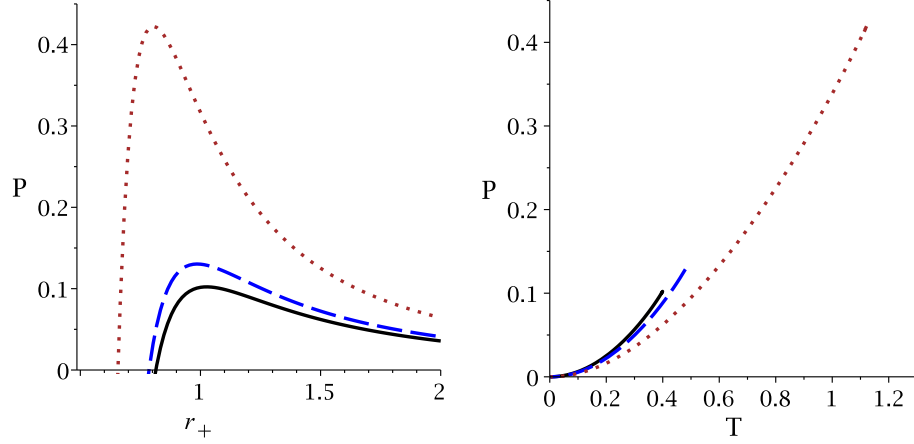

FIG. 11: P versus r_+ (left panel) and P versus T (right panel) for $c_1 = c_3 = c_4 = 2$, $c_2 = 3$ $k = 1$, $q = 1$, $m = 0.2$ and $n = 4$; $c_0 = 0.1$ (continues line), $c_0 = 1$ (dashed line) and $c_0 = 2$ (dotted line).
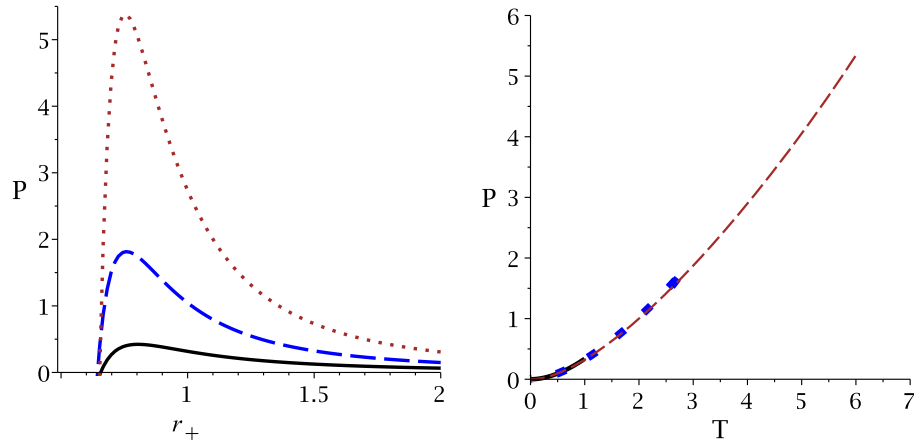

FIG. 12: P versus r_+ (left panel) and P versus T (right panel) for $c_0 = c_1 = c_3 = c_4 = 2$, $c_2 = 3$ $k = 1$, $q = 1$ and $m = 0.2$;
$n = 4$ (continues line), $n = 5$ (dashed line) and $n = 6$ (dotted line) in $P - r_+$ diagrams.
$n = 4$ (continues line), $n = 5$ (dotted line) and $n = 6$ (dashed line) in $P - T$ diagrams.

panel of Fig. 12). In addition, the length of coexistence curve is an increasing function of the massive gravity, c_0 and dimensions.

The massive parameter, m, is a measurement for the mass of the graviton. Here, we see that by increasing this parameter, the critical pressure and temperature increase while critical horizon radius decreases. This indicates that for massive graviton, black holes have phase transition in smaller horizon radius. On the other hand, considering massive graviton leads to increment of length of coexistence line between two different phases of smaller and larger black holes. Therefore, system in this case goes under second order phase transition in higher pressure and temperature. This effect highlights one of the differences between gravitational systems with massive gravitons and those with massless ones.

V.   CLOSING REMARKS

In this paper, we have reported a brief discussion regarding to the black hole solutions of massive gravity with a linear $U(1)$ gauge field. One of the interesting results of this paper was contribution of the massive gravity to number, type and place of horizons. It was shown that the mentioned three properties are highly sensitive to variation of the massive parameter and geometrical mass. It was pointed out that considering different values for the parameters will lead to different structures for the black holes. Although the massive terms could be up to $n + 2$ number, it is hard to study the total behavior of the solutions with this number of terms. Hence, for the sake of simplicity, we restricted our study to the fourth term.

From thermodynamical point of view, we have studied thermal stability, phase transition and geometrical thermo-dynamic behavior of the charged black holes in massive gravity. It was shown, in case of finding a critical massive parameter for both root and divergence points of the heat capacity, one will come across two sets of equations. In case of the root, the presence of all massive coefficients was only observed in the denominator of the obtained relation which showed that root of the heat capacity depends on these coefficients. Whereas for the critical massive parameter and divergence points of the heat capacity, one of the massive coefficients (c_1) had no contribution.

As for the physical/nonphysical point and second order phase transitions, it was pointed out there are three cases; i) only one bound point, ii) one bound point and one second order phase transition, and finally iii) one bound point and two second order phase transitions. These three situations are due to the contributions of massive part of solutions. In other words, considering the value of massive parameter, one of these cases may happen. Interestingly, smaller divergence point of the heat capacity for one dimension coincided with smaller divergence point of the other dimensions. The place of coincidences were different for every dimension. In other words, coincidence between two different dimensions took place for the specific value of massive parameter. For example, for $n = 4$ there are different values of the massive parameter (say m_1, m_2 and etc.) in which the horizon radius for smaller second order phase transition will be the same for $n = 5$, $n = 6$ and etc. Moreover, upon cancelling the electric charge of the solutions this characterized behavior was modified and the presence of second phase transition was vanished. This behavior highlights the role of the electric charge in thermodynamical behavior of the system.

Next, it was shown that thermal stability of the solutions is a function of bound and second order phase transition points. In other words, considering the number of the phase transition points, system may have different stable/unstable states.

At last, we employed geometrical approach for studying the thermodynamical behavior of the system. It was shown that employed thermodynamical metric in this paper, provided a suitable machinery for studying the phase transition of these black holes. In other words, regardless of bound point or second order phase transition, all the divergence points of Ricci scalar of the considered metric coincided with all root and divergence points of the heat capacity. It was also seen that characteristic behavior of the Ricci scalar enables one to recognize the bound point from the second order phase transitions.

In addition, using thermodynamical concept, a study regarding critical behavior of the system was conducted. The effects of different parameters on critical values and coexistence curve between two phases were investigated. The results regarding the massive parameter were investigated and considerable effects of m on the phase transition status were reported.

The main goal of this paper was investigation of geometrical thermodynamics and van der Waals like phase transitions in the context of a class of massive gravity. In order to obtain a general model of massive gravity, one may follow Stueckelberg mechanism and resuscitate the Goldstone modes which additionally come from breaking diffeomorphism. For example, in Ref. [151], it was shown that relaxation of the Poincare invariance leads to introduction of the large number of the options for generical massive gravity models. It is also worthwhile to consider a dilaton field in addition to Maxwell one and study its consequences. Moreover one can apply various nonlinear electrodynamics instead of Maxwell field in the context of massive gravity. Generalization of Einstein theory to modified and higher derivative gravities with a massive field is another interesting subject. In addition, since obtained black hole solutions

have various number and type of horizons, it will be interesting to study thermodynamical relations related to these horizons [152] and the possibility of the anti-evaporation property [71, 72]. In addition, following the approach of Ref. [75], it will be interesting to discuss the effective couplings of action (1) with scalars to obtain a consistent theory like bigravity. All these works could be addressed elsewhere.

Acknowledgments

[1] D. Lovelock, J. Math. Phys. **12**, 498 (1971).
[2] D. Lovelock, J. Math. Phys. **13**, 874 (1972).
[3] N. Deruelle and L. Farina-Busto, Phys. Rev. D **41**, 3696 (1990).
[4] P. Brax and C. van de Bruck, Class. Quantum Gravit. **20**, R 201 (2003).
[5] L. A. Gergely, Phys. Rev. D **74**, 024002 (2006).
[6] M. Demetrian, Gen. Relativ. Gravit. **38**, 953 (2006).
[7] M. Bouhmadi-Lopez and L. Chimento, Phys. Rev. D **82**, 103506 (2010).
[8] N. Cruz, S. Lepe, F. Pena and J. Saavedra, Eur. Phys. J. C **66**, 289 (2010).
[9] C. Brans and R. H. Dicke, Phys. Rev. **124**, 925 (1961).
[10] R. G. Cai and Y. S. Myung, Phys. Rev. D **56**, 3466 (1997).
[11] T. P. Sotiriou, Class. Quantum Gravit. **23**, 5117 (2006).
[12] M. H. Dehghani, J. Pakravan, and S. H. Hendi, Phys. Rev. D **74**, 104014 (2006).
[13] S. H. Hendi, J. Math. Phys. **49**, 082501 (2008).
[14] K. I. Maeda and Y. Fujii, Phys. Rev. D **79**, 084026 (2009).
[15] S. H. Hendi and R. Katebi, Eur. Phys. J. C **72**, 2235 (2012).
[16] X. Gao, Phys. Rev. D **90**, 081501 (2014).
[17] Y. Huang, Y. Gong, D. Liang and Z. Yi, Eur. Phys. J. C **75**, 351 (2015).
[18] M. Crisostomi, K. Koyama and G. Tasinato, JCAP **04**, 044 (2016).
[19] M. Akbar and R. G. Cai, Phys. Lett. B **648**, 243 (2007).
[20] J. C. C. de Souza and V. Faraoni, Class. Quantum Gravit. **24**, 3637 (2007).
[21] K. Atazadeh, M. Farhoudi and H. R. Sepangi, Phys. Lett. B **660**, 275 (2008).
[22] G. Cognola, E. Elizalde, S. Nojiri, S. D. Odintsov, L. Sebastiani and S. Zerbini, Phys. Rev. D **77**, 046009 (2008).
[23] C. Corda and H. J. Mosquera Cuesta, Europhys. Lett. **86**, 20004 (2009).
[24] T. P. Sotiriou and V. Faraoni, Rev. Mod. Phys. **82**, 451 (2010).
[25] S. H. Hendi, Phys. Lett. B **690**, 220 (2010).
[26] S. Nojiri and S. D. Odintsov, Phys. Rept. **505**, 59 (2011).
[27] S. H. Hendi, B. Eslam Panah and S. M. Mousavi, Gen. Relativ. Gravit. **44**, 835 (2012).
[28] S. H. Hendi, R. B. Mann, N. Riazi and B. Eslam Panah, Phys. Rev. D **86**, 104034 (2012).
[29] S. H. Hendi, Int. J. Theo. Phys. **53**, 4170 (2014).
[30] H. Zhang, D. J. Liu and X. Z. Li, Phys. Rev. D **90**, 124051 (2014).
[31] S. H. Hendi, B. Eslam Panah and C. Corda, Can. J. Phys. **92**, 76 (2014).
[32] Y. G. Miao, F. F. Yuan, Z. Z. Zhang, Int. J. Mod. Phys. D **23**, 1450093 (2014).
[33] S. H. Hendi, B. Eslam Panah and R. Saffari, Int. J. Mod. Phys. D **23**, 1450088 (2014).
[34] S. Capozziello, V. Galluzzi, G. Lambiase and L. Pizza, Phys. Rev. D **92**, 084006 (2015).
[35] S. Capozziello, S. J. Gabriele Gionti and D. Vernieri, JCAP **01**, 015 (2016).
[36] K. Bamba, Int. J. Geom. Meth. Mod. Phys. **13**, 1630007 (2016).
[37] S. N. Gupta, Phys. Rev. 96, 1683 (1954).
[38] S. Weinberg, Phys. Rev. 138, B988 (1965).
[39] S. Deser, Gen. Relativ. Gravit. 1, 9 (1970).
[40] D. G. Boulware and S. Deser, Ann. Phys. 89, 193 (1975).
[41] G. Dvali, G. Gabadadze and M. Porrati, Phys. Lett. B **485**, 208 (2000).
[42] G. Dvali, G. Gabadadze and M. Porrati, Phys. Lett. B **484**, 112 (2000).
[43] G. Dvali and G. Gabadadze, Phys. Rev. D **63**, 065007 (2001).
[44] E. A. Bergshoeff, O. Hohm and P. K. Townsend, Phys. Rev. Lett. **102**, 201301 (2009).
[45] S. F. Hassan and R. A. Rosen, JHEP **02**, 126 (2012).
[46] C. de Rham, G. Gabadadze and A. J. Tolley, Phys. Rev. Lett. **106**, 231101 (2011).

[47] C. de Rham, G. Gabadadze and A. J. Tolley, Phys. Lett. B **711**, 190 (2012).
[48] K. Hinterbichler, Rev. Mod. Phys. **84**, 671 (2012).
[49] M. Fierz, Helv. Phys. Acta **12**, 3 (1939).
[50] M. Fierz and W. Pauli, Proc. Roy. Soc. Lond. A **173**, 211 (1939).
[51] D. G. Boulware and S. Deser, Phys. Rev. D **6**, 3368 (1972).
[52] C. de Rham and G. Gabadadze, Phys. Rev. D **82**, 044020 (2010).
[53] S. F. Hassan and R. A. Rosen, JHEP **07**, 009 (2011).
[54] S. F. Hassan and R. A. Rosen, Phys. Rev. Lett. **108**, 041101 (2012).
[55] S. F. Hassan, R. A. Rosen and A. Schmidt-May, JHEP **02**, 026 (2012).
[56] Y. F. Cai, D. A. Easson, C. Gao and E. N. Saridakis, Phys. Rev. D **87**, 064001 (2013).
[57] S. Capozziello, M. De Laurentis, M. Paolella and G. Ricciardi, Int. J. Geom. Meth. Mod. Phys. **12**, 1550004 (2015).
[58] V. A. Rubakov and P. G. Tinyakov, Phys. Usp. **51**, 759 (2008).
[59] C. Bogdanos, S. Capozziello, M. De Laurentis and S. Nesseris, Astropart. Phys. **34**, 236 (2010).
[60] E. Tonni, JHEP **08**, 070 (2010).
[61] A. Ghodsi and M. Moghadassi, Phys. Lett. B **695**, 359 (2011).
[62] L. Berezhiani, G. Chkareuli, C. de Rham, G. Gabadadze and A. J. Tolley, Phys. Rev. D **85**, 044024 (2012).
[63] Y. S. Myung, Phys. Lett. B **730**, 130 (2014).
[64] F. Correa, M. Hassaine and J. Oliva, Phys. Rev. D **89**, 124005 (2014).
[65] E. Babichev and A. Fabbri, JHEP **07**, 16 (2014).
[66] E. Babichev and R. Brito, Class. Quantum Gravit. **32**, 154001 (2015).
[67] A. J. Tolley, D. J. Wu and S. Y. Zhou, Phys. Rev. D **92**, 124063 (2015).
[68] Y. Ohara, S. Akagi and S. Nojiri, Phys. Rev. D **92**, 023011 (2015).
[69] T. Kobayashi, M. Siino, M. Yamaguchi and D. Yoshida, [arXiv:1509.02096].
[70] P. Li, X. Z. Li and P. Xi, Phys. Rev. D **93**, 064040 (2016).
[71] T. Katsuragawa, Universe **1**, 158 (2015).
[72] T. Katsuragawa and S. Nojiri, Phys. Rev. D **91**, 084001 (2015).
[73] D. Langlois and A. Naruko, Class. Quantum Gravit. **29**, 202001 (2012).
[74] S. Nojiri and S. D. Odintsov, Phys. Lett. B **716**, 377 (2012).
[75] S. Nojiri, S. D. Odintsov and N. Shirai, JCAP **05**, 020 (2013).
[76] M. Fasiello and A. J. Tolley, JCAP **12**, 002 (2013).
[77] K. Bamba, A. N. Makarenko, A. N. Myagky, S. Nojiri and S. D. Odintsov, JCAP **01**, 008 (2014).
[78] K. Bamba, S. Nojiri and S. D. Odintsov, Phys. Lett. B **731**, 257 (2014).
[79] Y. F. Cai and E. N. Saridakis, Phys. Rev. D **90**, 063528 (2014).
[80] S. Pan and S. Chakraborty, Ann. Phys., **360**, 180 (2015).
[81] L. Heisenberg and A. Refregier, [arXiv:1604.07306].
[82] M. Baggioli and O. Pujolas, [arXiv:1604.08915].
[83] M. Baggioli and O. Pujolas, [arXiv:1601.07897].
[84] A. M. Garcia-Garcia, B. Loureiro and A. Romero-Bermudez, [arXiv:1606.01142].
[85] Y. Ling, P. Liu, J. P. Wu and Z. Zhou, [arXiv:1606.07866].
[86] B. Goutéraux, E. Kiritsis and W. J. Li, JHEP **04**, 122 (2016).
[87] D. Vegh, [arXiv:1301.0537].
[88] T. Andrade and B. Withers, JHEP **05**, 101 (2014).
[89] M. Taylor and W. Woodhead, Eur. Phys. J. C **74**, 3176 (2014).
[90] M. Baggioli and O. Pujolas, Phys. Rev. Lett. **114**, 251602 (2015).
[91] M. Baggioli and D. K. Brattan, [arXiv:1504.07635].
[92] R. G. Cai, Y. P. Hu, Q. Y. Pan and Y. L. Zhang, Phys. Rev. D **91**, 024032 (2015).
[93] J. Xu, L. M. Cao and Y. P. Hu, Phys. Rev. D **91**, 124033 (2015).
[94] S. H. Hendi, B. Eslam Panah and S. Panahiyan, JHEP **11**, 157 (2015).
[95] S. H. Hendi, S. Panahiyan and B. Eslam Panah, JHEP **01**, 129 (2016).
[96] S. H. Hendi, B. Eslam Panah and S. Panahiyan, JHEP **05**, 029 (2016).
[97] R. A. Davison, Phys. Rev. D **88**, 086003 (2013).
[98] M. Blake and D. Tong, Phys. Rev. D **88**, 106004 (2013).
[99] D. Kastor, S. Ray and J. Traschen, Class. Quantum Gravit. **26**, 195011 (2009).
[100] B. Dolan, Class. Quantum Gravit. **28**, 125020 (2011).
[101] G. W. Gibbons, R. Kallosh and B. Kol, Moduli, Phys. Rev. Lett. **77**, 4992 (1996).
[102] D. Rasheed, [arXiv:hep-th/9702087].
[103] N. Breton, Gen. Relativ. Gravit. **37**, 643 (2005).
[104] W. Y. Huan, Chin. Phys. B **19**, 090404 (2010).
[105] S. H. Hendi and M. H. Vahidinia, Phys. Rev. D **88**, 084045 (2013).
[106] R. A. Davison, K. Schalm and J. Zaanen, Phys. Rev. B **89**, 245116 (2014).
[107] S. H. Hendi, S. Panahiyan, B. Eslam Panah, Prog. Theor. Exp. Phys. **103E01** (2015).
[108] F. Weinhold, J. Chem. Phys. **63**, 2479 (1975).
[109] F. Weinhold, J. Chem. Phys. **63**, 2484 (1975).
[110] G. Ruppeiner, Phys. Rev. A **20**, 1608 (1979).

[111] G. Ruppeiner, Rev. Mod. Phys. **67**, 605 (1995).
[112] J. Shen, R. Cai, B. Wang and R. Su, Int. J. Mod. Phys. A **22**, 11 (2007).
[113] B. Mirza and M. Zamaninasab, JHEP **06**, 059 (2007).
[114] J. E. Aman, I. Bengtsson and N. Pidokrajt, Gen. Relativ. Gravit. **38**, 1305 (2006).
[115] T. Sarkar, G. Sengupta and B. N. Tiwari, JHEP **10**, 076 (2008).
[116] S. H. Hendi, S. Panahiyan, B. Eslam Panah and M. Momennia, Eur. Phys. J. C **75**, 507 (2015),
[117] S. H. Hendi, S. Panahiyan and B. Eslam Panah, Adv. High Energy Phys. **2015**, 743086 (2015).
[118] S. H. Hendi, S. Panahiyan, B. Eslam Panah and Z. Armanfard, Eur. Phys. J. C **76**, 396 (2016).
[119] S. H. Hendi, A. Sheykhi, S. Panahiyan and B. Eslam Panah, Phys. Rev. D **92**, 064028 (2015).
[120] S. H. Hendi, S. Panahiyan and B. Eslam Panah, Int. J. Mod. Phys. D **25**, 1650010 (2016).
[121] C. V. Johnson, Class. Quantum Gravit. **31**, 205002 (2014).
[122] B. P. Dolan, JHEP **10**, 179 (2014).
[123] E. Caceres, P. H. Nguyen and J. F. Pedrazab, JHEP **09**, 184 (2015).
[124] B. P. Dolan, Mod. Phys. Lett. A **30**, 1540002 (2015).
[125] S. H. Hendi, S. Panahiyan and R. Mamasani, Gen. Relativ. Gravit. **47**, 91 (2015).
[126] J. D. E. Creighton and R. B. Mann, Phys. Rev. D **52**, 4569 (1995).
[127] B. P. Dolan, Class. Quantum Gravit. **28**, 235017 (2011).
[128] D. Kubiznak and R. B. Mann, JHEP **07**, 033 (2012).
[129] R. G. Cai, L. M. Cao, L. Li and R. Q. Yang, JHEP **09**, 005 (2013).
[130] M. B. Jahani Poshteh, B. Mirza and Z. Sherkatghanad, Phys. Rev. D **88**, 024005 (2013).
[131] S. Chen, X. Liu and C. Liu, Chin. Phys. Lett. **30**, 060401 (2013).
[132] J. X. Mo and W. B. Liu, Eur. Phys. J. C **74**, 2836 (2014).
[133] D. C. Zou, S. J. Zhang and B. Wang, Phys. Rev. D **89**, 044002 (2014).
[134] W. Xu and L. Zhao, Phys. Lett. B **736**, 214 (2014).
[135] A. M. Frassino, D. Kubiznak, R. B. Mann and F. Simovic, JHEP **09**, 080 (2014).
[136] R. A. Davison, Phys. Rev. D 88, 086003 (2013).
[137] T. Q. Do, Phys. Rev. D **94**, 044022 (2016).
[138] S. Nojiri and Sergei D. Odintsov, Int. J. Mod. Phys. A **14**, 1293 (1999).
[139] S. Nojiri and Sergei D. Odintsov, Class. Quantum Gravit. **30**, 125003 (2013).
[140] S. Nojiri and Sergei D. Odintsov, Phys. Lett. B **735**, 376 (2014).
[141] J. Maldacena, Adv. Theor. Math. Phys. **2**, 231 (1998).
[142] E. Witten, Adv. Theor. Math. Phys. **2,** 253 (1998).
[143] S. W. Hawking, C. J. Hunter and M. M. Taylor-Robinson, Phys. Rev. D **59**, 064005 (1999).
[144] O. Aharony, S. S. Gubser, J. Maldacena, H. Ooguri and Y. Oz, Phys. Rep. **323**, 183 (2000).
[145] J. D. Beckenstein, Phys. Rev. D **7**, 2333 (1973).
[146] S. W. Hawking and C. J. Hunter, Phys. Rev. D **59**, 044025 (1999).
[147] C. J. Hunter, Phys. Rev. D **59**, 024009 (1999).
[148] S. W. Hawking, C. J. Hunter and D. N. Page, Phys. Rev. D **59**, 044033 (1999).
[149] R. B. Mann, Phys. Rev. D **60**, 104047 (1999).
[150] R. B. Mann, Phys. Rev. D **61**, 084013 (2000).
[151] L. Alberte, M. Baggioli, A. Khmelnitsky and O. Pujolas, JHEP **02**, 114 (2016).
[152] W. Xu, J. Wang and X. H. Meng, Galaxies, **3**, 53 (2015).
[153] The similar situation could be observed for generalization of the Einstein gravity to the Lovelock theory. The effective gravity in 4 dimensional case is Einstein theory. In 5 dimensions, the contributions of the Gauss-Bonnet terms appear and etc. But, it is a usual practice to study higher dimensional Einstein/Gauss-Bonnet gravity without consideration of the higher terms of Lovelock gravity. Here too, we have restricted our study up to $\mathcal{U}_4$.